

Thermal Trap for DNA Replication

Christof B. Mast and Dieter Braun*

Systems Biophysics, Physics Department, Center for Nanoscience, Ludwig Maximilians Universität München, Amalienstrasse 54, 80799 München, Germany

(Received 1 August 2009; published 7 May 2010)

The hallmark of living matter is the replication of genetic molecules and their active storage against diffusion. We implement both in the simple nonequilibrium environment of a temperature gradient. Convective flow both drives the DNA replicating polymerase chain reaction while concurrent thermophoresis accumulates the replicated 143 base pair DNA in bulk solution. The time constant for accumulation is 92 s while DNA is doubled every 50 s. The experiments explore conditions in pores of hydrothermal rock which can serve as a model environment for the origin of life.

DOI: 10.1103/PhysRevLett.104.188102

PACS numbers: 87.14.gk, 87.15.R–

Introduction.—Central to life is the buildup of structure. This requires the reduction of local entropy. As result, living systems have to be driven by nonequilibrium boundary conditions to agree with the second law of thermodynamics [1,2]. Modern cells use a complex metabolism and transport nutrients directionally across the cell membrane. But how could prebiotic molecules be accumulated with a nonequilibrium setting from a probably highly diluted ocean [3,4]?

A second central aspect is the replication of information-bearing molecules such as DNA or RNA. How could these molecules replicate and at the same time be hindered to diffuse out into the ocean? Ideally, evolution would be hosted by physical boundary conditions which drive a replication reaction and at the same time accumulate the replicated molecules against diffusion.

We experimentally show here a simple thermally driven system which replicates DNA by using a polymerase protein and simultaneously accumulates the replicated molecules in an efficient thermophoretic trap. The nonequilibrium driving is solely provided by a thermal gradient, possibly between warm volcanic rock and colder ocean water, a ubiquitous setting on the early earth [5,6].

This work brings together two lines of research. On the one hand, thermal convection [7] and thermophoresis [8] was initially shown to trap long DNA molecules under low salt conditions. Subsequently, it was pointed out theoretically that even single nucleotides should accumulate in centimeter-long cracks of hydrothermal rock [5] [Fig. 1(a)]. This approach was recently shown to accumulate lipids to form vesicles [9] and to trap 5 base pair DNA [10]. On the other hand, the exponential replication of DNA is provided in our experiments by the polymerase chain reaction (PCR) where DNA is periodically molten by a temperature oscillation and as a result, replicated with a primer-directed polymerase protein. Microthermal convection in various shapes was previously shown to provide the necessary temperature cycling for PCR [11–16] with exponential yield [12]. Under convection, DNA denatures

into two strands in the warm region [Fig. 1(b)] before it is shuffled by convection to colder regions where it can be replicated. Target inhibition [17,18] is circumvented by the periodic binding or unbinding protocols. This is essential for exponential replication, which itself is highly preferred in Darwinian evolution [19].

However, the convection geometries were not optimized for concurrent accumulation. Here, we show that both accumulation and replication of 143 base pair DNA can be implemented in an elongated single chamber. We used a glass capillary where the convection flow was driven by light driven microfluidics to achieve controllable experimental conditions [20,21]. The setting bodes well to select replicated molecules under continuous PCR using a superposed fluid flow.

Materials and methods.—We use a borosilicate capillary (VitroCom) with a rectangular cross section of $100\ \mu\text{m} \times 50\ \mu\text{m}$, embedded into immersion oil and sandwiched between an IR-transparent silicon wafer and a sapphire cover slip to enhance thermal gradients. The silicon wafer

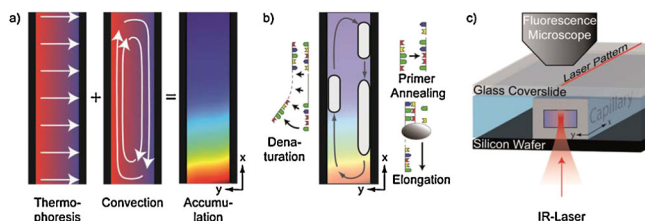


FIG. 1 (color online). Trapping and replicating DNA by thermal convection. (a) As molecules are directed to the right by thermophoresis, they are transported downward by the convection and accumulate at the bottom of the chamber. (b) Convection provides a temperature oscillation to periodically denature DNA with subsequent binding of short primers and replication by a polymerase protein. As a result, DNA is duplicated in each convection cycle. (c) A borosilicate capillary with rectangular cross section is heated symmetrically with an infrared laser. Directed scanning provides a convectionlike flow pattern due to light-driven microfluidics [20,21].

is cooled with Peltier elements (9502/065/018 M, Ferrotec) to 24 °C. The filled capillary is sealed on both ends by a reservoir of paraffin oil to prevent fluid drift. Imaging is realized with a fluorescence microscope (Axiotech Vario, Zeiss) using a high power cyan LED for illumination (Luxeon V Star, Lumiled lighting) and a CCD camera (Luca SDL-658M, Andor) using an air objective (20x, UPlanSApo NA = 0.75, Olympus).

Heating and thermoviscous flow is provided by an IR laser (1940 nm, 10 W, TLR-10-1940, IPG, Burbach) from the bottom. It is focused inside the capillary with a lens (C240TM, Thorlabs) after being deflected with scanning mirrors (6200-XY, Cambridge Technology). A heat bath (F20, Julabo) cools the microscope stage. Temperature imaging is provided with 50 μM of the dye BCECF [2',7'-bis-(2-carboxyethyl)-5-(and-6)-carboxyfluorescein, Invitrogen] in 10 mM TRIS-HCl buffer, 150 ms after switching on the laser and normalized against a previously taken cold picture [22,23]. The fluorescence decrease was calibrated by temperature dependent fluorescence measured in a fluorometer (Fluoromax-3, Horiba).

Fluid flow velocity was tracked with homogeneously distributed 1 μm fluorescent beads (F8888, Invitrogen) in the initial 5 seconds after the laser was switched on. Maximal recorded flow speed of $v_{\text{max}} = 70 \mu\text{m/s}$ indicated a chamber averaged velocity of $v = 2/3 v_{\text{max}} \approx 45 \mu\text{m/s}$. Finite element simulations were performed with FEMLAB (COMSOL), slightly modifying previous simulations [5]: the measured temperature profile replaced the previously linear temperature profile, and the flow pattern was approximated by gravitational flow (See Ref. [24]).

The PCR solution consists of 20 μl FastPCR master mix (Qiagen), 2 μl of 143 mer single stranded oligonucleotide template with random internal sequence at various concentrations, 2 \times 2 μl primer (sequences 5'-cccagctctgagcctcaagacgat-3', 5'-ggcttaaagcagaagtccaacca-3') with a final concentration of 500 nM, 2 μl 10 x SYBR Green I (Invitrogen), 2 μl 60 mg/ml BSA (biotin free, Roth), and 12 μl H₂O. PCR with 30 reaction cycles of denaturation at 96 °C (30 s), annealing at 53 °C (30 s), and elongation at 68 °C (30 s) were applied after 5 min of initial hot start at 95 °C. Reference PCR products were amplified in a RapidCycler (Idaho Technology) with 50 pM template DNA. DNA length and concentration were calibrated against standards with a 1.5% agarose gel.

Accumulation.—Short 143 base pair dsDNA accumulates by convection and thermophoresis. The convection flow is created optically with thermoviscous pumping [20,21] in an elongated pore geometry of size 100 $\mu\text{m} \times$ 1800 μm allowing for two mirror-symmetric convection rolls of width $a = 50 \mu\text{m}$ and mimicking gravitationally driven convection. Thermophoretic drift $j_T = -D_T c \nabla T$ is characterized by the thermodiffusion coefficient D_T , driving the DNA along the horizontal thermal gradient ∇T [Fig. 2(c)]. This concentration bias towards the cold sides is accumulated to the chamber center by the fluid flow [Fig. 2(d)].

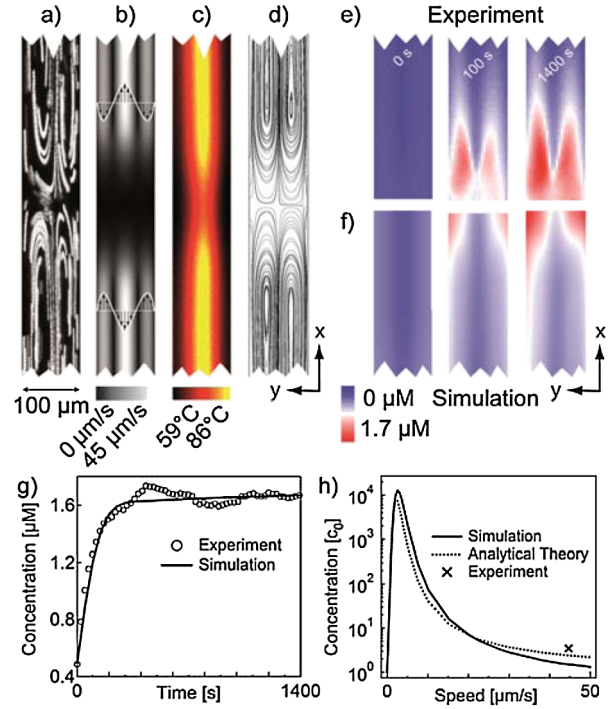


FIG. 2 (color online). Accumulation of DNA. (a) In the chamber center, the convection flow was tracked with 1 μm particles. The chamber averaged flow speed is 45 $\mu\text{m/s}$. (b) The corresponding flow profile for the finite element simulation. (c) The temperature profile was measured using a temperature dependent dye [8]. (d) Molecular trajectories by the superposition of fluid flow and thermophoresis. (e) Fluorescence images show the DNA accumulation over time. (f) The concentration pattern over time is reasonably described theoretically. (g) The kinetics of central accumulation is well described theoretically. (h) Optimal convection speed for accumulation is around 2.5 $\mu\text{m/s}$. The experimental conditions favor faster PCR replication under reduced accumulation.

Above concentration mechanism is counterbalanced by diffusion, resulting in a concentration plateau after 300 s as measured by the intercalating DNA dye SYBR Green I [Fig. 2(e)]. Concentration increases to 1.7 μM of DNA, up from the initial 0.49 μM concentration. The experimental result is described reasonably well by a time dependent simulation using the measured temperature and flow profile [Fig. 2(f)].

The accumulation kinetics in the center is shown in Fig. 2(g). A hydrodynamic time constant $\tau_{\text{Trap}} = 2l/v = 80 \text{ s}$ for accumulation can be estimated from the convection flow and the chamber length l and agrees well with the experimentally found accumulation time of 92 s. Further accumulation is kinetically limited by diffusive refilling at the outer boundaries of the flow [10]. The steady state accumulation of a thermogravitational column can be described by [25]

$$\frac{c_{\text{Trap}}}{c_0} = \exp\left(\frac{q/120}{1 + q^2/10080} S_T \Delta T r\right), \quad (1)$$

with q defined as

$$q = \frac{\Delta T \alpha g \rho_0 a^3}{6 \eta D}, \quad (2)$$

where c_{Trap}/c_0 denotes the ratio of the DNA concentration at the accumulation center to the outer boundaries, $S_T = D_T/D$ the Soret coefficient, D the ordinary diffusion coefficient, $r = l/a$ the aspect ratio of the convection, η the viscosity of the solvent, ρ_0 the density of the solvent, α the volume expansion of the solvent, and g the local acceleration due to gravity. The maximum convection flow velocity in a 2D chamber is given by [25]

$$v = \frac{\Delta T \alpha g \rho_0}{6 \eta} a^2 \frac{3}{64}. \quad (3)$$

By eliminating g , we obtain the accumulation ratio depending on the convection flow v

$$\frac{c_{\text{Trap}}}{c_0}(v) = \exp\left(\frac{504 v a S_T \Delta T r D}{2835 D^2 + 128 v^2 a^2}\right). \quad (4)$$

It matches well with the finite element simulation [Fig. 2(h)]. Although flow and temperature gradient were created by an infrared laser, the conditions do not differ significantly from gravitational driving.

Accumulation and PCR.—In the same setting, the DNA molecules follow the fluid flow and are cycled through a temperature difference of 27 K with an average cycling time based on the convection flow of $\tau_{\text{cycle}} = 2l/v = 80$ s. This is an upper bound since the inclusion of thermophoretic drift tends to shorten the cycle time. Based on the size and charge of DNA [5,8], we expect the preferential accumulation of DNA. However, even if all the components of the PCR mix accumulate, they would still thermally cycle, albeit on shorter molecular trajectories.

The PCR reaction is driven by the melting of the 143 mer at 86 °C and primer binding and replication at 59 °C. The generated DNA is accumulated by the trap dynamics. With template DNA, we find an increased fluorescence in the trap, but only background fluorescence is detected without template [Fig. 3(a)]. For the concentration of replicated but not yet trapped DNA, we expect a raise in fluorescence given by a sigmoidal curve with doubling time τ_{doubling} and amplification delay $t_{1/2}$ [26]

$$c_{\text{PCR}}(t) = \frac{c_{\text{max}}}{1 + \exp[\ln(2)(t_{1/2} - t)/\tau_{\text{doubling}}]}. \quad (5)$$

The initial single-stranded DNA is immediately elongated to double-stranded DNA by the polymerase in the first round. The reaction therefore effectively starts with double-stranded DNA. No significant contribution to the fluorescence signal is expected as its concentration is 500-fold and 85.000-fold lower than the final replicated and accumulated product [Fig. 3(c)]. The DNA which replicated homogeneously at time $t - \tau$ is accumulated by the trap with time delay τ . So the concentration of trapped PCR product will follow

$$c_{\text{TrappedPCR}}(t) = \int_0^t c_{\text{Trap}}(\tau) \dot{c}_{\text{PCR}}(t - \tau) d\tau. \quad (6)$$

The shape of the concentration increase leads for template containing probes to $\tau_{\text{doubling}} = 74$ s. A reduced template DNA concentration delays the replication of PCR. We find $t_{1/2}^A = -8$ s for $c_A = 3500$ pM of initial DNA and $t_{1/2}^B = 380$ s for $c_B = 20$ pM. From this, we infer a doubling time of $\tau_{\text{doubling}} = \ln 2(t_{1/2}^B - t_{1/2}^A)/\ln(c_A/c_B) \approx 50$ s which fits the data equally well [Fig. 3(c), solid line]. As discussed [26], this evaluation using $t_{1/2}$ should be more reliable than the fitting of τ_{doubling} from the sigmoidal shape. The fact that τ_{doubling} is slightly smaller than τ_{cycle} might indicate a shortening of the DNA trajectories or a possible cotrapping of the PCR mix.

Controls.—The thermophoretic characteristics of amplified DNA were compared against DNA amplified in a standard cycler. Standard methods are not available to verify the length of the replicated DNA due to the low product volumes in the capillary. Lengths of the expected 143 mer, shorter 86 mer, and longer 1530 mer were created by standard PCR and confirmed using gel electrophoresis [Fig. 4(a)].

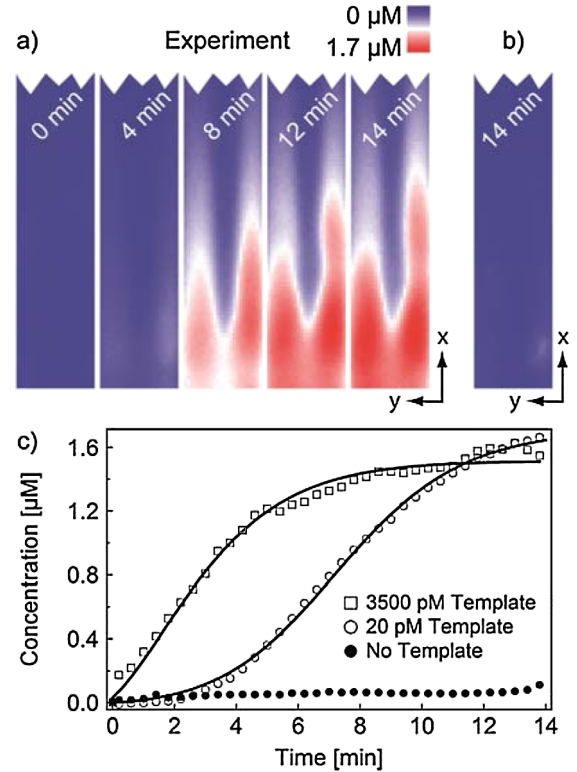


FIG. 3 (color online). Replication Trap. (a) Accumulation of PCR product by convection and thermophoresis, visualized by SYBR Green fluorescence. (b) No DNA is found without template DNA. (c) Center concentration over time and fits with Eq. (6). Delays of replication due to different template concentrations allow us to infer the replication doubling time with $\tau_{\text{doubling}} = 50$ s.

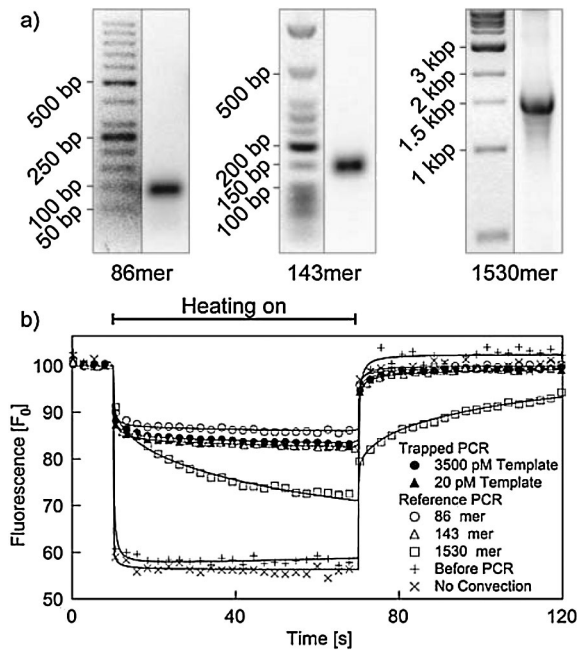


FIG. 4. Verification of the product. (a) Gel electrophoresis of product from a standard PCR cycler. Different primers yield product lengths of 86, 143, and 1530 base pairs. (b) In the capillary, the product is identified using thermophoresis [27,28]. Upon local heating with a laser spot, DNA is locally depleted. The amplified product matches the 143 base pair product and is well bracketed by 86 mer and 1530 mer product.

A low power IR laser spot was temporarily generated with a Gaussian temperature profile with $T_{\max} = 9$ K and width $\sigma = 100$ μm in the capillary in the accumulated spot after the PCR has finished. Thermophoretic depletion and backdiffusion was recorded by fluorescence [Fig. 4(b)]. From the time trace, we infer the diffusion coefficient D and the thermodiffusion coefficient D_T [8,27,28]. The product of the replication trap agrees with the 143 mer in both $D = 23$ $\mu\text{m}^2/\text{s}$ and $D_T = 0.26$ $\mu\text{m}^2/\text{s K}$ (solid line) and is bracketed by the shorter and longer DNA signal. Longer DNA with 1530 base pairs is clearly distinguishable and yields $D = 1.7$ $\mu\text{m}^2/\text{s}$ and $D_T = 0.24$ $\mu\text{m}^2/\text{s K}$ whereas the 86 mer yields $D = 25$ $\mu\text{m}^2/\text{s}$ and $D_T = 0.15$ $\mu\text{m}^2/\text{s K}$. No product shows a large temperature dependence with a fast diffusion kinetics indicating unbound SYBR Green. We find these characteristics before PCR or for a symmetric scanning pattern that heats without fluid flow [Fig. 4(b)].

Discussion and outlook.—We showed that temperature gradients across elongated pores can drive both replication and accumulation of short DNA. Our experiment mimics conditions in pores of hydrothermal vents [5], but also has biotechnological relevance for HPLC or capillary electrophoresis. It bodes well for continuous feeding of PCR by a slow capillary flow while trapping the replicated DNA at a fixed position. The setting yields 1700 DNA replications

within 24h, considerably faster than for example *E. coli* with 70 replications per day.

We thank Hubert Kramer for reading the manuscript. Financial support from the NanoSystems Initiative Munich, the International Doctorate Program NanoBioTechnology, and the LMU Initiative Functional Nanosystems is gratefully acknowledged.

*dieter.braun@lmu.de

- [1] J. S. Wicken, *J. Theor. Biol.* **72**, 191 (1978).
- [2] D. Braun and A. Libchaber, *Phys. Biol.* **1**, P1 (2004).
- [3] K. Dose, *BioSystems* **6**, 224 (1975).
- [4] S. J. Mojzsis, T. M. Harrison, and R. T. Pidgeon, *Nature (London)* **409**, 178 (2001).
- [5] P. Baaske *et al.*, *Proc. Natl. Acad. Sci. U.S.A.* **104**, 9346 (2007).
- [6] W. Martin and M. J. Russell, *Phil. Trans. R. Soc. B* **358**, 59 (2003).
- [7] D. Braun and A. Libchaber, *Phys. Rev. Lett.* **89**, 188103 (2002).
- [8] S. Duhr and D. Braun, *Proc. Natl. Acad. Sci. U.S.A.* **103**, 19678 (2006).
- [9] I. Budin, R. J. Bruckner, and J. W. Szostak, *J. Am. Chem. Soc.* **131**, 9628 (2009).
- [10] F. M. Weinert and D. Braun, *Nano Lett.* **9**, 4264 (2009).
- [11] M. Krishnan, V. M. Ugaz, and M. A. Burns, *Science* **298**, 793 (2002).
- [12] D. Braun, N. L. Goddard, and A. Libchaber, *Phys. Rev. Lett.* **91**, 158103 (2003).
- [13] E. K. Wheeler *et al.*, *Anal. Chem.* **76**, 4011 (2004).
- [14] D. Braun, *Mod. Phys. Lett. B* **18**, 775 (2004).
- [15] M. Hennig and D. Braun, *Appl. Phys. Lett.* **87**, 183901 (2005).
- [16] N. Agrawal, Y. A. Hassan, and V. M. Ugaz, *Angew. Chem., Int. Ed.* **46**, 4316 (2007).
- [17] G. von Kiedrowski, *Angew. Chem., Int. Ed.* **98**, 932 (1986).
- [18] A. Luther, G. Brandsch, and G. von Kiedrowski, *Nature (London)* **396**, 245 (1998).
- [19] E. Szathmary and I. Gladkih, *J. Theor. Biol.* **138**, 55 (1989).
- [20] F. M. Weinert, J. A. Kraus, T. Franosch, and D. Braun, *Phys. Rev. Lett.* **100**, 164501 (2008).
- [21] F. M. Weinert and D. Braun, *J. Appl. Phys.* **104**, 104701 (2008).
- [22] P. Baaske, S. Duhr, and D. Braun, *Appl. Phys. Lett.* **91**, 133901 (2007).
- [23] M. L. Cordero, E. Verneuil, F. Gallaire, and C. N. Baroud, *Phys. Rev. E* **79**, 011201 (2009).
- [24] See supplementary material at <http://link.aps.org/supplemental/10.1103/PhysRevLett.104.188102> for the FEMLab 3.1 file of the numerical simulation.
- [25] P. Debye, *Ann. Phys. (Leipzig)* **428**, 284 (1939).
- [26] S. Swillens, B. Dessars, and H. E. Housni, *Anal. Biochem.* **373**, 370 (2008).
- [27] S. Duhr, S. Arduini, and D. Braun, *Eur. Phys. J. E* **15**, 277 (2004).
- [28] P. Reineck, C. J. Wienken, and D. Braun, *Electrophoresis* **31**, 279 (2010).